

Dimuon trigger characterization for the study of the multiquark candidate $X(3872)$ at LHC Run 3 with the CMS experiment

N. PALMERI⁽¹⁾(²)

⁽¹⁾ *INFN, Sezione di Roma - Roma, Italy*

⁽²⁾ *Dipartimento di Fisica, Università di Roma - Roma, Italy*

received 31 January 2024

Summary. — The analysis of the $B^0 \rightarrow X(3872)K_S^0$ production channel of the tetraquark candidate $X(3872)$, performed on CMS data acquired during LHC Run 3, is here presented. We characterised the performance of the new low- p_T dimuon trigger configuration implemented in Run 3 used for the analysis and estimated its impact on signal selection efficiency, which suggests a significant improvement with respect to Run 2 triggers. Finally, preliminary results on the control channel are presented, showing good agreement between data and Monte Carlo and resulting in a branching ratio measurement compatible with the world average. The present analysis has yet to be fully validated by the CMS Collaboration, therefore only preliminary results will be presented.

1. – Introduction

Quantum chromodynamics, the theory governing strong interactions in the Standard Model of particle physics, predicts the existence of various classes of bound states composed of quarks, named hadrons, which have all found experimental validation over the past century. Until recently, all discovered hadrons fitted into the picture described by the traditional quark model, which only contemplates two categories: mesons, consisting of a quark and anti-quark pair, and baryons, composed of three quarks. The discovery of the first in a series of exotic resonances, which did not conform to this classification, marked the onset of a new era in exotic hadron spectroscopy. $X(3872)$, a multiquark charmed resonance with a mass of 3.872 GeV discovered by the Belle experiment in 2003 [1], was the inaugural member of this intriguing group. Although initially believed to be a charm quark-antiquark bound state, *i.e.*, a charmonium state, its production and decay properties defied this classification.

Despite its discovery occurring two decades ago, a debate persists regarding the inner structure of $X(3872)$. Presently, several alternative hypotheses on its structure have emerged, with two garnering most of the experimental support. The first posits that $X(3872)$ is a loosely bound $D^0\bar{D}^{*0}$ molecule, with one compelling argument being the small mass difference between $X(3872)$ and the combined masses of the two supposedly constituent mesons. Alternatively, another possibility is that $X(3872)$ is a compact

tetraquark state, composed of two quarks and two anti-quarks, hence lying outside of the conventional quark model, yet not explicitly ruled out by it.

Given the current inability of experimental evidence to definitively favour one scenario over the other, in order to shed light on the puzzle surrounding the nature of the $X(3872)$ resonance, it is critical to reconstruct as many decay and production channels as possible with the highest precision allowed. My work contributes to the ongoing efforts by investigating the $B^0 \rightarrow X(3872)K_S^0$ channel, in which $X(3872)$ is produced from the decay of a B^0 meson with associated production of a K_S^0 meson, with full decay chain:

$$B^0 \rightarrow X(3872)K_S^0 \rightarrow J/\psi \rho K_S^0 \rightarrow \mu^+ \mu^- \pi^+ \pi^- \pi^+ \pi^-.$$

This analysis has been conducted on data collected by the Compact Muon Solenoid (CMS) experiment, hosted at the Large Hadron Collider (LHC), an accelerator capable of colliding protons at a center-of-mass energy up to $\sqrt{s} = 13.6$ TeV. CMS has dedicated substantial resources to the study of the physics of B mesons, including the investigation of rare decay channels, such as, in recent times, $B_s^0 \rightarrow X(3872)\phi$ [2]. Similarly to our channel, such a decay describes the associated production of $X(3872)$ with a light hadron from a B meson decay, which is sensitive to $X(3872)$'s inner structure.

The dedication of the collaboration to the study of heavy-flavour physics has culminated during Run 2 —*i.e.*, the second period of data taking since LHC started operation, lasting from 2015 to 2018— with the introduction of a dedicated data acquisition strategy aimed at increasing the statistics available to the study of such decays, namely B -parking [3]. With Run 3, started in 2022, this strategy has been expanded with the development of new trigger configurations aimed at increasing the sensitivity of the experiment to previously inefficiently studied topologies, including the one under scrutiny in this analysis.

Among the newly introduced trigger algorithms, the new low-transverse-momentum (from here onwards low- p_T) dimuon trigger proved to be the best suited one to study the $B^0 \rightarrow X(3872)K_S^0$ channel, targeting the $\mu^+ \mu^-$ pair produced in the $X(3872)$ decay. The analysis has been thus performed on data collected with such a trigger strategy in 2022 by the CMS experiment during Run 3 of LHC, amounting to an integrated luminosity of $L = 29.61 \text{ fb}^{-1}$, with an enhanced sensitivity with respect to previous studies.

1.1. Analysis strategy. – The investigation of the signal channel consists in the measurement of the branching ratio $\text{BR}(B^0 \rightarrow X(3872)K_S^0)$. However, in order to ease the experimental procedure, it is convenient to avoid measuring its absolute value, but rather normalise it by the branching ratio of a suitably defined *control channel* (opposed to our *signal* channel), such that common factors —and, hence, some of the experimental systematic uncertainties on the final value— may cancel out.

In order for the cancellation to occur, the control channel must be chosen with a topology and kinematics as similar as possible to the signal. This led to the selection of the $B^0 \rightarrow \psi(2S)K_S^0$ process, where the $X(3872)$ is replaced by the $\psi(2S)$ excited charmonium resonance. The similarity in kinematics is guaranteed by the small mass difference between $m_{X(3872)} \approx 3.872$ GeV and $m_{\psi(2S)} \approx 3.686$ GeV, with $\Delta m \approx 186$ MeV; in terms of topology, instead, both the signal and control channel share the same final state.

Given the relation $N = \mathcal{L} \cdot \sigma \cdot \mathcal{B} \cdot \varepsilon$ between the measured number of events N and the product of all branching ratios \mathcal{B} entering the decay chain (with \mathcal{L} being the integrated luminosity, σ the cross-section and ε the signal selection efficiency) we can express the

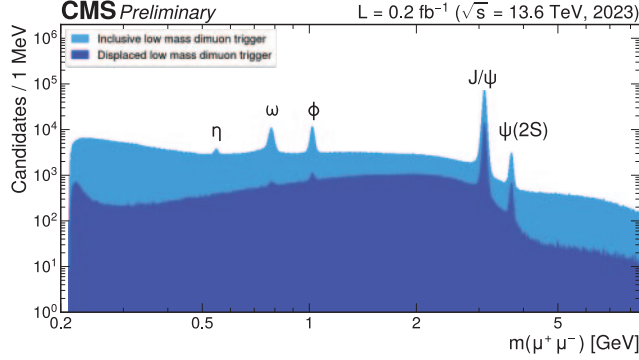


Fig. 1. – Dimuon invariant mass distribution for events collected with Run 3 low-mass dimuon triggers. Several light hadronic resonances are visible (η , ω , ϕ), as well as two of the lightest charmonium states (J/ψ , $\psi(2S)$) [4].

quantity of interest, based on the considerations outlined earlier, as follows:

$$R = \frac{\text{BR}(B^0 \rightarrow X(3872)K_S^0) \cdot \text{BR}(X(3872) \rightarrow J/\psi \pi^+ \pi^-)}{\text{BR}(B^0 \rightarrow \psi(2S)K_S^0) \cdot \text{BR}(\psi(2S) \rightarrow J/\psi \pi^+ \pi^-)} = \frac{N_{X(3872)}}{\varepsilon_{X(3872)}} \cdot \frac{\varepsilon_{\psi(2S)}}{N_{\psi(2S)}},$$

where the last equality decomposes R in the values which were explicitly measured. As anticipated, several common factors (*e.g.*, L , σ) cancel out in the ratio. For ease of notation, we have represented the measured number of signal events after the full selection $N_{X(3872)}$, while the efficiency in detecting such events is denoted as $\varepsilon_{X(3872)}$; the same convention is adopted for the control channel with $N_{\psi(2S)}$, $\varepsilon_{\psi(2S)}$.

Once the signal selection strategy, optimised to maximise signal significance, has been devised, we can extract $N_{X(3872)}$, $N_{\psi(2S)}$ by fitting the m_{B^0} mass spectrum in each channel —computed as the invariant mass of all final state particles in the decay chain, *i.e.*, $m(\mu\mu\pi\pi\pi\pi)$ — with an appropriately chosen function modelling both the signal and background components; the normalisation N of the signal component stands for the number of events in the fitted channel.

The signal selection efficiencies $\varepsilon_{\psi(2S)}$, $\varepsilon_{X(3872)}$ descend instead from all selection steps applied on data, starting from trigger request. It is hence first necessary to characterise its performance, starting with the measurement of its efficiency as a function of the most relevant kinematic variables associated to the muons.

2. – Dimuon trigger performance in Run 3

In Run 3, the increased bandwidth allocated to B -parking allowed more inclusive triggers to be developed, reducing the requirements imposed on the selected particles and enlarging the low- p_T phase space —which is the kinematical region of interest for B meson decays— as much as possible. The most inclusive of the newly introduced trigger configurations is the low- p_T dimuon trigger; the $\mu\mu$ mass spectrum obtained from events selected with this algorithm is shown in fig. 1, which can now include a variety of Standard Model resonances decaying to a dimuon final state with a single trigger request, up to the $\psi(2S)$.

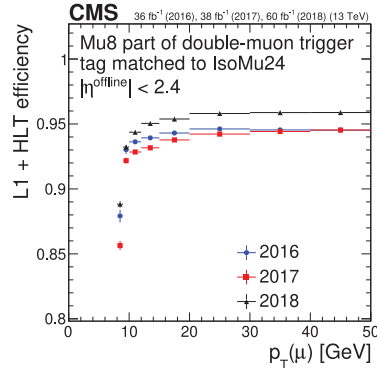


Fig. 2. – Trigger efficiency in detecting the probe muon for dimuon Run 2 triggers with respect to muon p_T for 2016, 2017, and 2018 [5].

2.1. Tag and probe. – Evaluating the dimuon trigger efficiency on data poses a non-trivial challenge in the task of constructing a dataset containing only events with (at least) two unbiased muons to be selected. This issue can be overcome by means of the *tag and probe* technique, which exploits di-object tight resonances (*i.e.*, with a small decay width Γ with respect to their mass m) to construct samples containing one unbiased particle. The mass of the chosen tight resonance dictates the accessible muon kinematical region: since we are interested in low- p_T muons ($p_T \lesssim 10$ GeV), the lightest charmonium state, J/ψ , has been thus exploited for this study.

The efficiency study starts from a data sample acquired with a single-muon trigger, which we will refer to as our reference trigger. The muon requested by the reference trigger, defined as the *tag* muon, is biased due to the cuts imposed on it by the trigger firing request, and is not suitable for efficiency evaluation. However, we can apply an offline selection to these events in order to only select those which contain a J/ψ decaying into 2 muons. Given the decaying resonance and the tag muon presence, we can be significantly confident that there is a second muon—defined as the *probe* muon—without imposing any further direct cuts, hence introducing less bias through this procedure.

Given this sample of probe muons, we can study the trigger efficiency by evaluating the fraction of probe muons passing the selection over the total number of muons. In order to exclude any combinatorial or residual background, we fit the dimuon invariant mass $m(\mu\mu)$ distribution to extract the J/ψ signal component. This process can be then repeated as a function of the probe kinematics, such as its p_T and pseudorapidity η , in order to better characterise the trigger response.

An illustrative example of the efficiency trend we can expect as a function of the probe’s p_T is depicted in fig. 2 for a similar Run 2 dimuon trigger (imposing, however, a higher cut in muon p_T). As we can see, the efficiency drops to 0 for p_T values below the threshold value requested by the trigger—in this case, equal to 8 GeV—and rises up to a saturation value close to 1 for higher p_T values.

2.2. Expected impact on analysis. – As the analysis is still currently under development, the results of the just outlined efficiency evaluation strategy are not public yet. However, we can estimate the impact of the new trigger on the analysis on the basis of the comparison in overall signal yield between Run 2 and Run 3 trigger configurations in a similar channel. In fig. 3, the yield of B^0 particles decaying as $B^0 \rightarrow J/\psi K_S^0$ obtained by using Run 3 *vs.* Run 2 triggers is shown.

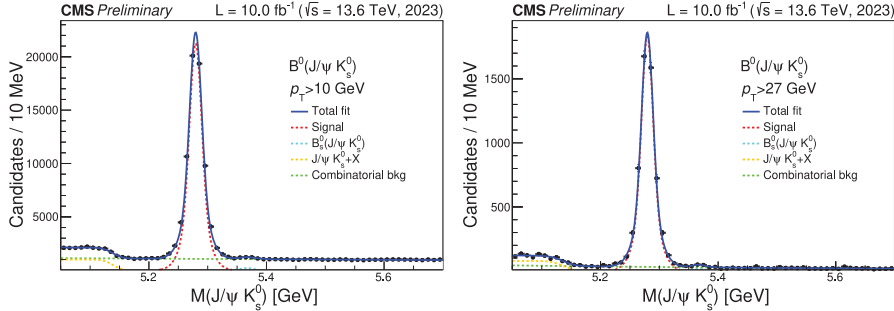


Fig. 3. – Comparison of signal yield of the $B_d^0 \rightarrow J/\psi K_S^0$ decay channel in events acquired with Run 3 and Run 2 inclusive triggers. The left plot corresponds to data collected by the Run 3 trigger, while the right plot is obtained with the Run 2 inclusive trigger. The signal yield is about 12 times larger with the Run 3 trigger [4].

The newly introduced trigger leads to a 12-fold increase in signal yield with respect to the equivalent inclusive Run 2 trigger. As a result, we can expect a similar improvement to propagate to the precision with which we can determine the final $B^0 \rightarrow X(3872)K_S^0$ branching ratio.

3. – Study of the $B^0 \rightarrow X(3872)K_S^0$ channel

Having successfully characterised the trigger performance, the next step in the analysis involved the extraction of the number of events in each channel $N_{X(3872)}$, $N_{\psi(2S)}$ according to the strategy outlined above. Particular focus was then dedicated to the estimation of the signal selection efficiencies $\varepsilon_{X(3872)}$, $\varepsilon_{\psi(2S)}$.

3.1. Signal selection efficiency from Run 2 to Run 3. – The signal selection efficiencies $\varepsilon_{\psi(2S)}$, $\varepsilon_{X(3872)}$ have been evaluated on Monte Carlo, decomposing them into the partial efficiencies associated to each selection step —here also including trigger application.

Preliminary results obtained using the Run 3 dimuon trigger have been compared to the corresponding values extracted in the Run 2 data analysis, which suggest an improvement in signal selection efficiency in both control and signal channels comparable to the signal yield increase observed in the $B^0 \rightarrow J/\psi K_S^0$ channel shown in fig. 3, *i.e.*, an approximately 10-fold increase.

To illustrate the expected shape of the $X(3872)$ spectrum and the signal-to-background ratio obtained with the new Run 3 triggers, we can refer to fig. 4, displaying the $m(\mu\mu\pi\pi)$ invariant mass distribution obtained from events selected by the new low- p_T dimuon trigger with an additional requirement of displacement between the proton-proton collision point and the $X(3872)$ decay vertex —which is indeed often appreciable due to the long lifetime characterizing the initial B meson, hence making the two results comparable.

3.2. Results. – Since the analysis has yet to be fully validated, the signal region —here referring to events reproducing the desired decay chain and containing a $\mu\mu\pi\pi$ resonance with an invariant mass comparable to the $X(3872)$ mass— is blinded, meaning no optimisation on the selection procedure can be done by using the signal region as

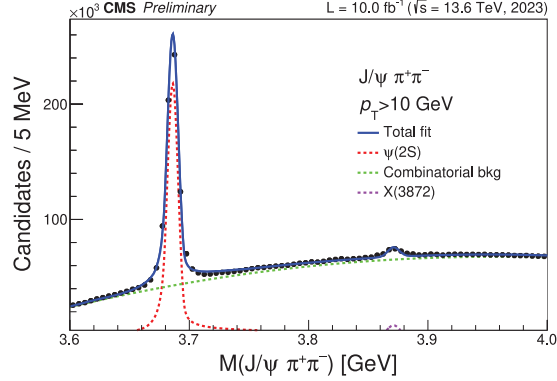


Fig. 4. – $m(\mu\mu\pi\pi)$ invariant mass distribution in events selected with the low- p_T , displaced Run 3 dimuon trigger. Both the $\psi(2S)$ and $X(3872)$ resonances are visible over background [4].

reference in order to avoid introducing any bias. Consequently, the only available results refer to the $\psi(2S)$ control region.

We have observed good agreement between data and Monte Carlo, suggesting effective control over the simulation stage of the analysis. Additionally, as an intermediate validation step, extracting the control channel branching ratio $\text{BR}(B^0 \rightarrow \psi(2S)K_S^0)$ yields a value compatible with the world average, taking into account statistical uncertainty only. This suggests the analysis procedure does not introduce any appreciable bias in the branching ratio estimation, which we expect to also extend to the signal channel.

4. – Conclusions

The performance of the new B -parking low- p_T dimuon trigger introduced in Run 3 has been characterised, with a specific focus on its potential benefits to the $X(3872)$ analysis outlined above. Studies on its efficiency performed using the tag and probe strategy and comparison between signal yield in Run 2 and Run 3 in the similar channel $B^0 \rightarrow J/\psi K_S^0$ point to a significant improvement in signal selection efficiency in the analysed $B^0 \rightarrow X(3872)K_S^0$ channel.

Preliminary results from the analysis of the $B^0 \rightarrow \psi(2S)K_S^0$ control channel performed on the data acquired with the new dimuon trigger suggest a good agreement between data and Monte Carlo. Furthermore, the measurement of $\text{BR}(B^0 \rightarrow \psi(2S)K_S^0)$ yields a value compatible with the current world average, indicating the absence of any appreciable bias in the branching ratio estimation procedure. This outcome makes the investigation of the $X(3872)$ signal channel a promising avenue for further analysis.

REFERENCES

- [1] BELLE COLLABORATION, *Phys. Rev. Lett.*, **91** (2003) 262001.
- [2] CMS COLLABORATION, *Phys. Rev. Lett.*, **125** (2020) 152001.
- [3] CMS COLLABORATION, CMS-DP-2019-043.
- [4] CMS COLLABORATION, CMS NOTE-2023/007.
- [5] CMS COLLABORATION, *JINST*, **16** (2021) P07001.